Slovak Geol. Mag., 8, 1(2002), 49 – 63

Cooling and uplift trajectories of the Malé Karpaty Variscan Basement (West Carpathians)

MARIAN DYDA

Department of Mineralogy and Petrology, Comenius University, Mlynská dolina, SK-84215 Bratislava.
e-mail: dyda@fns.uniba.sk

Abstract. In the Malé Karpaty the Variscan regional metamorphic recrystallisation temperatures (570-620 °C) and pressures (4.7-6.1 Kbar) in Bratislava massive differ significantly from contact periplutonic processes in Modra massive. The approximative P-T trajectories express the first order tectonic motion and specific uplift conditions of the particular basement blocks. The culmination whole rock reaction paths have steep slopes (dP/dT ≈ 89-121 bar/K) and later compositional changes modified dominantly by diffusion processes run during decompression cooling (dP/dT ≈ 62-68 bar/K). These trajectories are consistent with regional metamorphic environment and the metamorphic culmination was associated with granitoidic polyphase magmatism. The post culmination multiple heating events are absent and mineral assemblages reflect the one thermal culmination event. The annealing estimates indicate that ca. 0.10-0.53 garnet mass fraction was transferred during cooling. These estimates are good cooling rate indicators and the values testify about the regional metamorphic processes. The calculated depth and heating rate data ($4*10^{-5}$ °C/y) may provide corresponding burial rate of 1-2 km/Ma. Cooling rate data calculated from garnet diffusional zonality (~ 4.7-94 °C/Ma) assess the approximate exhumation rate at 0.2-3.8 km/Ma. The data confirm different cooling scenarios for tectonicaly controlled rapid uplift end erosion. The orogenic block transport, stacking and restructuring occurred in the Variscan era and the tectonic complexity in the region was also shaded by complicated tectono deformation development in the Alpine period.

Key words: geothermobarometry, reaction slope, cooling rate, metamorphic trajectories, West Carpathians.

Introduction

The complicated nappe structure of the Western Carpathian mountain range was recognized as early as 1898 and 1903 by Viktor Uhlig and later in 1903 by M. Lugeon. Since works of Andrusov (1936, 1968), Andrusov et al., (1973) it has been accepted that two upper Mesozoic sedimentary sequences form groups of nappes, lower the Krížna nappe and the upper the Choč nappe. The lowermost Mesozoic sequences create the Cover formation underlying nappe formations and overlying the crystalline basement complexes. Recently, the crystalline basement complexes and their sedimentary cover rocks are considered to be allochthonous (Leško et al.,1980, Maheľ,1983, Maheľ,1986, Bezák et al.,1998, Vozárová, 1998).

The „core mountains" are situated in the outer zone of the Western Carpathians segment. They crop out within the unfolded Paleogene and Neogene rocks and exhibit dome structure with the crystalline core, tectonical overprinting by Mesozoic events and a distinct style of Paleogene sedimentation. There are some deviations from more central „core mountains" that , in some cases, suggest facies and tectonic similarities with the Eastern Alpine segment.

The largest tectonic superunit of the Central Western Carpathian is the Tatricum. It forms the lowermost basement substratum of the „core mountains", laying between the Klippen Belt in north and other basement superunits further south, the Veporicum and the Gemericum (Putiš, 1991, Plašienka et al., 1991).

The Malé Karpaty have a prominent position in the crystalline basement studies. The basement rocks are represented by paragneisses, orthogneisses, amphibolites and other high grade metamorphic rock complexes later inruded by Variscan granitoidic rocks.

Geological Setting

The Malé Karpaty (M.K.) play a specific and important role in the Eastern Alpine and Western Carpathian relationship and correlation as they bear some typical geological features of both mountain systems, but they have a prevailing Carpathian influence (Maheľ, 1983).

The Variscan postkinematic granitoidic rocks are the predominant constituent of the M.K. crystalline complex. They form two separate massifs, the Bratislava and Modra massifs, separated by a 4-8 km wide zone of schists. According to the genetic I/S classification, the M.K. granitoid rocks are transitional. Their geochemical fea-

tures are suggestive of being I-Caledonian type. The Bratislava granitoid massif clearly shows a tendency towards S-type granitoids (Cambel & Vilinovič, 1987).

The age of contact metamorphism dated on contact metamorphic biotites, is within the range of age determination of Bratislava granitoidic massif intrusion, 298 - 354 m.y. (Bagdasarjan et al., 1983). The biotite pairs Rb/Sr isochron gives age of 344 ± 3 m.y. (Cambel et al., 1990b). This age determination is considered to be the age of Bratislava granitoid massif intrusion.

The sedimentary overburden was regionally metamorphosed before granitoid rocks intruded and periplutonic processes became dominant in some areas. The metamorphic process took place during the late Variscan era (Cambel & Valach, 1956; Cambel et al., 1990a,b). The spatial relationship and metamorphic zonality exists in some areas only as rudimentary remnants. In other places the complete metamorphic zonality was preserved (Broska & Janák, 1985; Dyda & Miklóš, 1993).

Disturbances of the Variscan metamorphic structures caused by Alpidic tectonic movements destroyed the original metamorphic zonation. This is evident from appearance of index minerals, irregularity of dehydration reaction progress and reaction volume changes in metapelites and paragneisses of the periplutonic zones (Dyda and Miklóš 1993). These processes do not progress continually in the profiles and at some places have no relation to the distance from granitoidic contact. This serves as a petrological argument for distinquishing between paraautochthonous and alochthonous metamorpfic zones in the area and support the concept of tectonic destruction of the Variscan periplutonic zones and the basement as a whole (Dyda, 1997).

Earlier tectonic concepts (Cambel, 1952,1954) were not in favour of any Alpidic orogenic activity in the crystalline basement complexes, and only development of Alpidic fault retrograde processes were considered. However, recent tectonometamorphic and petrological research indicates complex tectonic and structural development of this core mountain mass (Dyda, 1977, 1980a, 1980b, 1994, 1999, 2000; Cambel et al., 1981; Korikovskij et al., 1984; Miklóš, 1986, 1987). This requires the assumption of several superimposed nappe units consisting of pre-Alpine crystalline basement with its Mesozoic cover (Putiš, 1987, 1991; Plašienka et al., 1991; Marko et al., 1991).

Complex structures of the mountains reflect their complicated development, which started hundreds of kilometers southwards, and the remnants of Variscan mountains were overridden by Paleo-Alpine nappe piles. Their structures were modified by back-thrusts and transpressional tectonics (Plašienka, 1989; Plašienka et al., 1991).

The reconstruction of the Hercynian orogenic cycle in Western Carpathians is complicated because of the presence of the Alpine tectonic overprinting. Fragments of Hercynian structure were incorporated into new paleoalpine units. To reconstruct their original tectonic position, the elimination of younger tectonic effects is needed as well as the analysis of their development (Bezák, 1993). Thus, due to the tectonic disturbances of the Variscan orogen, it is still unclear whether the crystalline complexes in some „core mountains" are in an autochthonous position.

The present petrologic study is focused on metamorphic reaction extent, geothermobarometry, whole rock reaction paths,cooling estimates and metapelitic rocks uplift trajectories with the aim to describe and approximate specific petrological processes that bring new aspects of metamorphic development of this important geological area. The contribution of this paper is to place a larger amount of information relevant to the determination of uplift trajectories on a more accessible format than was previously available.

Methods and data

The initial mineral constituents of the studied metapelites have been approximated by protolith calculations (Dyda & Miklóš, 1993) that determines protolithic presence of quartz, plagioclase, K-feldspar, chlorite, illite, montmorillonite, calcite, ankerite, rodochrosite and rutil in the protolitic sediments. The present modal composition of studied paragneisses is given in Tab.1.

*Table 1. Chemical *and modal composition of the representative Tatric basement paragneisses from the Malé Karpaty.*

Sample	*KB-2.*	*KB-3.*	*KB-5.*	*17.*
SiO_2	62.77	65.26	56.05	62.16
TiO_2	0.82	0.69	1.03	0.81
Al_2O_3	17.27	16.55	19.59	17.04
Fe_2O_3	4.24	3.58	4.72	3.82
FeO	3.60	2.67	5.01	4.10
MnO	0.18	0.13	0.28	0.15
MgO	2.35	1.46	2.58	2.18
CaO	1.77	2.48	2.04	1.49
Na_2O	2.88	3.84	3.10	2.46
K_2O	2.38	1.85	2.82	2.60
H_2O^+	1.18	0.65	1.47	1.79
Σ	99.45	99.16	98.69	98.60
Number of ions in rock on 160 hydrous oxygen basis				
Fe^{3+}	2.853	2.406	3.270	2.578
Fe^{2+}	2.692	1.994	3.857	3.075
Mn	0.136	0.098	0.218	0.113
Mg	3.132	1.943	3.540	2.913
X_{Fe}**	0.629	0.683	0.654	0.651
Modal composition				
Quartz	34.1	31.1	24.3	38.0
Plagioclase	32.5	39.1	35.1	26.1
Biotite	27.5	27.6	33.8	29.9
Muscovite	0.6	0.5	2.1	2.5
Garnet	3.5	1.2	1.8	1.6
Staurolite	0.7	-	0.4	1.3
Sillimanite	0.9	0.2	2.3	0.4
Opaque ***	0.2	0.3	0.2	0.2

*Wet chemical analyses. Analyst: E.Waltzel;**X_{Fe}= ΣFe/(Fe^{3+}+Fe^{2+}+Mn+Mg) ***dominantly ilmenite.

With increasing metamorphic grade the rock experienced transformations via unspecified progressive reaction. It is to notice that no reaction rests from earlier metamorphic stages indicating pre-culmination trajectory have been observed as e.g. inclusions in garnets. Thus, the major whole rock reactions encountered in the rocks represent terminal stability of staurolite which occurs at culmination temperature and pressure in sillimanite stability field. Staurolite remove from the assemblages is accompanied with progressive growth of garnet and sillimanite in the assemblage St+Ms+Bt+Grt+Sil+Pl+Qtz, where important kyanite rests are consumed and eventually disappear. During decompression stages kyanite → sillimanite reaction boundary is crossesd and kyanite presence is replaced by fibrolitic sillimanite. Kyanite is almost completely resorbed and significant unresorbed kyanite rests remain only in some assemblages (Fig.1.). Existing homogenous garnet porphyroblasts posses no kyanite inclusions (Fig.2.).

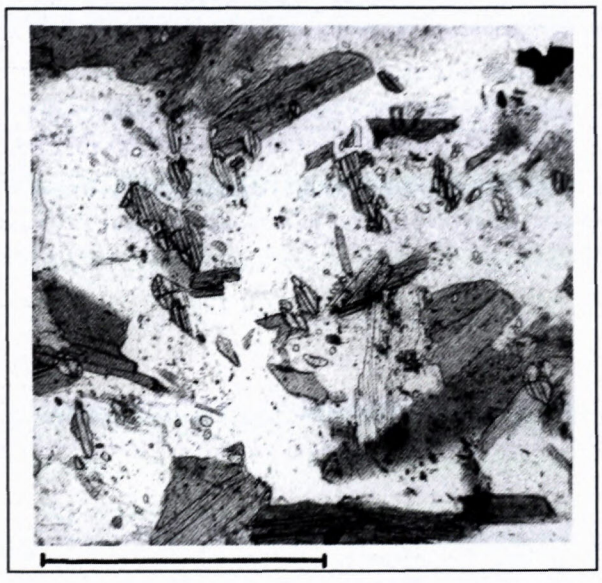

Fig. 1. Higher pressure kyanite relics in the Tatric basement paragneisses from Malé Karpaty, first described by Dyda (1999), prove the higher pre culmination metamorphic pressures and are consistent with the steep whole rock reaction path during decompression. (Scale bar = 0.5 mm).

The evaluation of metamorphic trajectories primarily relies on geothermobarometric data based on chemical composition of equilibrium mineral assemblages. However, the portion of the trajectory may be eradicated by later higher temperature processes. Thermodynamic modelling of the zoned minerals e.g. garnet (Spear & Selverstone,1983) provides reliable P-T trajectory reconstruction in fulfilling the fundamental assumption that the zonning observed in the garnet is the product of growth of continuous equilibrium reaction and that zonning has not been later modified by thermal diffusional processes. Simultaneously the assemblage present during garnet growth must be known. This imperative requirement can not always be fulfilled and in addition, mineral dise-

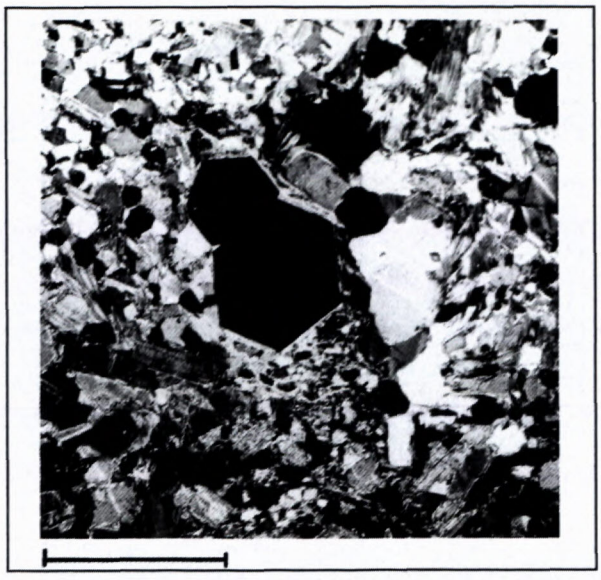

Fig. 2. Idioblastic garnet morphology and its progressive growth in sillimanite stability field is consistent with calculated staurolite decomposition reaction (A1) and with no microscopic decomposition features clearly indicates a quenched assemblage and a rapid decompression uplift process.(Sample 17., Scale bar = 0.5 mm).

disequilibrium features form, during the P-T changes. Thus the inherited mineral disequilibrium features from previous metamorphic stages coexist as the consequence of slow mineral reactions rate.

JEOL Superprobe 733 and JEOL 840 microprobe served for mineral analyses. The operating conditions were 20 kV accelerating voltage, specimen current of 15-20 μA and beam diameter 1-2 μm. For sodic plagioclase and muscovite the beam diameter was increased to 5-7 μm to avoid sodium loss. In order to obtain the representative chemical analyses of the centre of zoned minerals (garnet, plagioclase), only the largest grains assumed to be in equilibrium contact with surrounding minerals were selected and analysed from polished thin section.

In each sample 3-6 grains of each mineral have been analysed in two to three locations to test the homogeneity of the grain. Total iron has been calculated as ferrous. Fe^{3+} in garnets and biotites was not calculated as the accuracy depends highly on all of the elements analysed, H_2O, Al^{IV},Al^{VI} content, compositional limits and on the structural balance. Anyhow, the numerical approach of Shumacher (1991, 1997) may be useful in this respect. The chemical compositions of the coexisting garnets, biotites, muscovites, plagioclasses and staurolites of the equilibrium mineral assemblages are given in Tab. 2.

In the thermobarometrical approach some differences occurred steaming from different calibrations of the particular mineral reactions. Uncertainties and their estimates that have appeared in the literature usually adopt values of $\sigma T = 50\ ^{\circ}C$ and $\sigma P = 1$ Kbar. Many samples from single location reflect this general consensus (e.g. Ferry, 1980; Ghent & Stout, 1981) based on the reproducibility of the P-T data (Hodges & Crowley, 1985).

Table 2. Chemical composition of coexisting minerals in Tatric basement paragneisses.

Garnet analyses								
M.K.	**17c**	**17r**	**KB2c**	**KB2r**	**KB3c**	**KB3r**	**KB5c**	**KB5r**
SiO_2	37.36	35.90	37.46	36.35	37.03	36.67	37.12	37.35
TiO_2	0.04	0.00	0.03	0.03	0.02	0.01	0.08	0.01
Al_2O_3	21.43	21.17	21.68	21.26	20.98	20.75	21.25	20.73
FeO	29.15	30.87	30.12	31.35	30.15	30.14	27.68	31.22
MnO	8.71	7.25	5.55	6.39	7.36	8.09	9.03	6.41
MgO	2.59	2.65	3.41	3.08	2.66	2.36	2.81	2.53
CaO	1.30	1.29	1.70	1.42	1.83	1.94	1.97	1.48
Σ	100.58	99.13	99.95	99.88	100.03	99.96	99.94	99.73
Cations / 12 oxygens								
Si	2.995	2.940	2.994	2.945	2.991	2.978	2.988	3.022
Ti	0.002	0.000	0.001	0.002	0.001	0.001	0.004	0.000
Al	2.025	2.043	2.043	2.031	1.997	1.987	2.017	1.977
Fe	1.954	2.114	2.013	2.124	2.036	2.047	1.863	2.113
Mn	0.591	0.502	0.375	0.438	0.503	0.556	0.616	0.439
Mg	0.309	0.323	0.406	0.372	0.320	0.285	0.337	0.305
Ca	0.111	0.113	0.145	0.123	0.158	0.168	0.170	0.128
Plagioclase analyses								
M.K.	**17c**	**17r**	**KB2c**	**KB2r**	**KB3c**	**KB3r**	**KB5c**	**KB5r**
SiO_2	59.80	59.03	61.35	61.39	61.14	60.91	61.45	61.52
Al_2O_3	23.82	24.40	24.53	25.10	24.54	24.30	23.56	24.03
FeO	0.05	0.15	0.15	0.01	0.10	0.08	0.10	0.10
CaO	5.25	5.91	5.80	6.41	5.50	5.80	5.12	5.41
Na_2O	10.98	10.62	8.49	7.96	8.54	8.80	8.85	8.66
K_2O	0.05	0.05	0.08	0.07	0.14	0.05	0.06	0.05
Σ	99.95	100.16	100.40	100.94	99.96	99.94	99.14	99.77
Cations / 8 oxygens								
Si	2.686	2.653	2.716	2.701	2.716	2.712	2.750	2.736
Al	1.261	1.292	1.280	1.302	1.285	1.275	1.243	1.260
Fe^{2+}	0.001	0.005	0.005	0.000	0.003	0.002	0.003	0.003
Ca	0.252	0.284	0.275	0.302	0.261	0.276	0.245	0.257
Na	0.956	0.925	0.728	0.679	0.735	0.759	0.768	0.746
K	0.002	0.002	0.004	0.003	0.007	0.002	0.003	0.002
Biotite analyses								
M.K.	**17c**	**17r**	**KB2c**	**KB2r**	**KB3c**	**KB3r**	**KB5c**	**KB5r**
SiO_2	35.18	34.97	36.28	36.03	35.44	35.69	36.73	36.20
TiO_2	1.60	1.38	2.06	2.08	1.89	2.10	1.91	1.80
Al_2O_3	19.39	20.14	19.68	20.16	19.55	20.05	19.79	19.71
FeO	19.83	19.97	18.17	18.62	19.98	18.60	17.71	19.81
MnO	0.14	0.14	0.02	0.18	0.27	0.14	0.21	0.11
MgO	9.66	10.34	9.17	9.29	8.82	8.96	9.65	9.41
Na_2O	0.48	0.52	0.46	0.21	0.14	0.24	0.44	0.32
K_2O	8.37	7.43	8.91	8.52	9.14	9.70	8.96	8.09
Σ	94.68	94.89	94.75	95.08	95.23	95.46	95.40	95.45
Cations / 22 anhydrous oxygens								
Si	5.374	5.301	5.486	5.427	5.401	5.395	5.502	5.450
Ti	0.183	0.157	0.234	0.235	0.216	0.239	0.215	0.203
Al	3.493	3.599	3.508	3.580	3.512	3.577	3.495	3.498
Fe	2.534	2.532	2.298	2.345	2.546	2.354	2.219	2.494
Mn	0.018	0.017	0.002	0.022	0.034	0.020	0.026	0.014
Mg	2.199	2.336	2.066	2.085	2.003	2.020	2.154	2.111
Na	0.144	0.152	0.134	0.061	0.041	0.070	0.129	0.093
K	1.632	1.437	1.719	1.637	1.777	1.872	1.712	1.553

Table 2. (continued)

Muscovite analyses.					Staurolite analyses.				
M.K	**17c**	**17r**	**KB5c**	**KB5r**		**17c**	**17r**	**KB5c**	**KB5r**
SiO_2	46.49	46.36	47.06	46.98	SiO_2	27.41	27.42	27.27	27.33
TiO_2	0.14	0.12	0.47	0.53	TiO_2	0.69	0.60	0.56	0.60
Al_2O_3	36.35	36.34	35.79	35.44	Al_2O_3	52.89	53.25	54.49	52.98
FeO	1.05	1.08	1.35	1.65	FeO	12.67	12.99	12.25	12.66
MgO	0.54	0.57	0.50	0.51	MnO	0.08	0.04	0.03	0.07
CaO	0.00	0.02	0.02	0.03	MgO	1.86	1.64	1.81	1.78
Na_2O	1.52	1.53	1.38	1.24	ZnO	0.58	0.58	0.73	0.74
K_2O	8.85	8.85	8.60	8.97					
Σ	94.94	94.87	95.17	95.35	Σ	96.18	96.52	97.14	96.16
Cations / 22 anhydrous oxygens					Cations / 46 anhydrous oxygens				
Si	6.151	6.141	6.205	6.206	Si	7.672	7.706	7.591	7.708
Ti	0.013	0.011	0.046	0.052	Ti	0.146	0.126	0.117	0.127
Al	5.670	5.675	5.563	5.519	Al	17.627	17.642	17.882	17.616
Fe	0.116	0.119	0.148	0.182	Fe	2.995	3.053	2.851	2.986
Mg	0.106	0.112	0.098	0.100	Mn	0.019	0.009	0.007	0.016
Ca	0.000	0.002	0.002	0.004	Mg	0.783	0.686	0.750	0.748
Na	0.389	0.393	0.352	0.317	Zn	0.121	0.121	0.150	0.154
K	1.493	1.495	1.446	1.511					

*Table 3. Metamorphic recrystallisation temperatures of representative Malé Karpaty Tatric basement paragneisses.**

Sample			ln K_D	T	F&S	N&H	G&S
KB-	17	c	1.701	570	587	602	610
		r	1.797	545	551	566	568
KB-	02	c	1.491	628	666	687	648
		r	1.626	589	610	626	610
KB-	03	c	1.610	594	619	641	639
		r	1.813	541	546	568	587
KB-	05	c	1.675	577	596	619	614
		r	1.764	553	562	579	580

* Using equilibrium calibrations of: T - Thompson (1976); F & S - Ferry a Spear (1978); N & H - Newton a Haselton (1981); G & S - Ganguly a Saxena (1984).
c - culminatilon temperatures of metamorphic recrystallization.
r - retrograde closure temperatures.

Geothermometric data based on the garnet rims and adjacent coexisting biotite at multiple mutual junctions approximate the retrograde closure temperature. Garnet cores and matrix biotites yielded an higher temperature related to a metamorphic thermal culmination. In metapelitic rocks with high biotite/garnet modal ratio the post culmination Fe-Mg mass balance reactions slightly change the biotite peak composition (Crowley, 1991).

Different sets of calibrated mineral equilibria were used to infer the P-T data of metamorphic thermal culmination and retrograde closing conditions to determine the position of the rock sample in the P-T coordinates (Tab. 3., 4., 5.). The accurate position of the sample in the P-T space may be uncertain, still within the limits of 2σ, but this is of lesser importance if regional metamorphic and tectonic interpretation of the obtained data are taken into consideration.

The lowest variance mineral assemblages of the studied paragneisses include St, Bt, Grt, Ms, Pl, Ilm, Sil, Qtz. The metamorphic whole rock reaction among these minerals is represented formally by a system of linear equations for components chosen. This algebraic approach may include all components and simultaneously exclude degenerative composition relations among minerals in the assemblage. Each composition balance for given component in the assemblage is defined as

$$A_i = \nu_1 X_{1i} + \nu_2 X_{2i} + \nu_3 X_{3i} + \ldots \nu_n X_{ni} \qquad (1.)$$

where ν - is the stoichiometric koeficient, X_i - element concentration in the mineral and A_i - is the concentration of the same element in the reference mineral. The linear equation e.g. for Si and Al in the simplified metapelitic KMFASH system in the assemblage Chl+Ms+Grt+Bt+Qtz is then expressed:

$$0 = \nu_{Chl}\, Si_{Chl} + \nu_{Ms}\, Si_{Ms} + \nu_{Qtz}\, Si_{Qtz} + \nu_{Grt}\, Si_{Grt} + \nu_{Bt}\, Si_{Bt} \quad (2.)$$

$$0 = \nu_{Chl}\, Al_{Chl} + \nu_{Ms}\, Al_{Ms} + \nu_{Qtz}\, Al_{Qtz} + \nu_{Grt}\, Al_{Grt} + \nu_{Bt}\, Al_{Bt} \quad (3.)$$

The formulated set of chemical composition of minerals participating in particular metamorphic reaction thus devides and quantifies the minerals of the assemblage on the reaction reactants and products. Critical importance still has the appearence of equilibrium rock structure.

The mineral abundance in paragneisses (Tab.1.) and their compositions (Tab.2.) can thus be arranged in numerical form to express the whole rock metamorphic reactions. Reaction stoichiometry gives consequently a P-T vector determining the slope $dP/dT = \Delta S/\Delta V$ of the culmination reaction paths A1, B1 and specifies the reaction slopes of closing retrograde exchange processes as the reactions A2, B2 in the studied samples (Tab. 6.).

KB-5. Core

1 St + 0.263 Ms + 0.970 Pl + 1.730 Qtz = 8.135 Sil +
+ 1.398 Grt + 0.223 Bt + 0.156 Ilm + 1.765 H_2O
reaction path - slope dP/dT = 121.7 bar/K. (A1)

*Table 4. Metamorphic recrystallisation pressures of representative Malé Karpaty basement paragneisses.**

Sample		aAn	aGr	G	G&S	H&C	N&H	P&H	P&H^P
KB -	17c	0.3298	0.0412	4.8	4.1	4.7	4.4	5.3	4.8
	r	0.4107	0.0411	3.6	3.6	3.8	3.1	4.1	4.0
KB -	2c	0.4083	0.0557	6.0			5.9	5.9	5.9
	r	0.5053	0.0449	3.8			3.3	4.2	3.7
KB -	3c	0.4142	0.0574	5.7			5.3	6.1	5.7
	r	0.4806	0.0604	4.6			3.8	4.9	4.4
KB -	5c	0.3920	0.0625	5.9	5.1	5.7	5.5	6.4	5.2
	r	0.4458	0.0476	4.0	4.0	4.2	3.4	4.4	4.1

* Using equilibrium pressure calibrations of: G - Ghent et al .(1979), G&S - Ghent & Stout (1981), H&C - Hodges & Crowley (1985), N&H - Newton & Haselton (1981), P&H - Powell a Holland (1988),P&H^P- THERMOCALC, Powell & Holland (1988, 1998). Activity of anorthite (aAn) and grossular (aGr) is based on formulation of Newton & Haselton (1981).
c - pressures of metamorphic recrystallisation at thermal maximum, r - pressures at retrograde temperature minimum.

*Table 5. Composition and pressure characteristics of representative paragneisses in the Bratislava granitoidic massif area based on the calibration of Hoisch (1990, 1991).**

Composition characteristics:									
Sample			lnK$_D$1	lnK$_D$2	lnK$_D$3	lnK$_D$4	lnK$_D$5	lnK$_D$6	ΔV(J/bar)
KB	17	c	5.3558	3.6983	4.1446	0.8392	9.9161	4.9437	- 0.2790
		r	5.7870	4.0361	4.6026	1.0438	10.676	5.4237	- 0.2812
KB	05	c	4.5859	2.9750	3.4652	0.5296	8.8068	3.9774	- 0.1696
		r	5.5383	3.8270	4.4224	0.9816	10.322	5.1887	- 0.2569
Pressure characteristics P(bar):									
Sample			P1	P2	P3	P4	P5	P6	K&N**
KB-	17	c	4784	4754	4519	4830	4724	4631	4917
		r	3800	3762	3633	3988	3687	3601	3621
KB-	05	c	5821	5725	5653	5659	6044	5831	6164

R^*_1 1/3 Pyrope + 2/3 Grossular + Eastonite + 2 Quartz = 2 Anorthite + Phlogopite
R_2 1/3 Almandine + 2/3 Grossular + Siderophylite + 2 Quartz = 2 Anorthite + Annite
R_3 1/3 Pyrope + 2/3 Grossular + Muscovite +2 Quartz = 2 Anorthite + MgAlCeladonite
R_4 1/3 Phlogopite +1/3 Grossular + 2/3 Muscovite+2Quartz=Anorthite+ MgAlCeladonite
R_5 Pyrope + Grossular + Muscovite = 3 Anorthite + Phlogopite
R_6 Almandine + Grossular + Muscovite = 3 Anorthite + Annite
K&N**comparison calibration according to Koziol & Newton (1988).

Table 6. Entropies S_T (J K^{-1} mol^{-1}) and volumes V_M (cm^3 mol^{-1}) of coexisting phases at metamorphic peak culmination and closing retrograde temperatures and pressures used for metamorphic reaction P-T slopes calculations.*

Sample	KB - 5.				KB - 17.			
	S_{601}	S_{568}	V_M^C	V_M^R	S_{592}	S_{557}	V_M^C	V_M^R
Plagioclase	489.07	482.88	100.23	100.24	492.21	478.53	101.21	100.23
Biotite	877.69	862.84	151.86	152.17	875.94	816.03	152.86	151.91
Muscovite	740.38	722.60	138.98	139.31	740.26	715.87	138.88	137.95
Staurolite	2816.46	2745.51	447.17	447.74	2796.13	2719.98	447.19	447.74
Garnet	816.32	797.07	115.92	115.65	813.98	786.20	115.85	114.98
Ilmenite	228.13	223.03	31.68	31.69	226.75	221.27	31.68	31.69
Sillimanite	269.09	261.89	49.86	49.86	267.12	259.44	49.86	49.86
Quartz	106.09	103.23	22.68	22.69	105.33	102.26	22.69	22.69
H_2O	227.41	-	21.45		227.01	-	22.66	

*Entropy and volume of the particular phase has been calculated according to Spear & Rumble (1986). Molar volume of the solid solution phase is given by the expression $V_M = \Sigma\, x_i V_i$, where x_i is the mole fraction of the i-th component and V_i is its molar volume. Entropy of mineral solid solution at given temperature is expressed as $S_M^T = \Sigma\, x_i S_i - n\, R\, \Sigma\, x_i \ln x_i$, where n is the site multiplicity. For plagioclase series albite and anorthite have been considered as the solid solution end members, for biotites - phlogopite and annite, muscovites - muscovite and paragonite, staurolite - MgStaurolite and FeStaurolite, garnets - almandine, spesartine, pyrope and grossular. The internally consistent thermodynamic database of Holland - Powell (1998) has been used

KB-5. Rim
1 St + 985.1 Sil + 427.4 Ilm + 73.7 Bt + 2889 Qtz = 75.75 Ms + 245.4 Grt + 1133 Pl
reaction path - slope dP/dT = 62.9 bar/K. (A2)

KB-17. Core
1 St + 0.323 Ms + 0.555 Pl + 2.431 Qtz = 8.037 Sil + + 1.266 Grt + 0.296 Bt + 0.159 Ilm + 1.773 H_2O
reaction path - slope dP/dT = 89.3 bar/K. (B1)

KB-17. Rim
1 St + 48.67 Ms + 172.9 Grt + 669.8 Pl = 643.6 Sil + + 307.4 Ilm + 50.67 Bt + 1658 Qtz
reaction path - slope dP/dT = 68.5 bar/K. (B2)

Generally considered, rock decompression accompanied with heating gives a stoichiometric reaction with negative reaction slope and decompression during cooling is characterised by a positive one. The changes in modal abundance and textural features of mineral growth or reactant consumption along this P-T vector determine the reaction extent as well (Fig.3.). Different reaction rock stoichiometry thus permits numerical solution for rock cooling along different reaction path on the post culmination metamorphic trajectories. The calculated reaction stoichiometry compared with microscopic study of the samples thus assures the resemblance to the calculated whole rock reaction that actually run in the rock. Both petrological approaches are consistent in the studied assemblages and the constraints are placed on the calculated P-T path (Fig.4.).

Processes that effect modal changes and element distribution among minerals are strictly path dependent and reflect P-T conditions along the reaction path. The dehydration maximum of rock thus coincides with temperature culmination of rock P-T trajectory and the equilibrium forming peak metamorphic assemblage (Fig.5.).

However, different bulk rock composition of the studied rocks (Tab.1.) attributes different reaction extent of these changes during each rock reaction P-T history and thus the changes in the modal proportions of minerals with respect to growth or consumption specify each rock trajectory.

The studied garnets are the products of growth during metamorphic culmination whole rock reaction and existing zoning is the product of diffusional processes after progressive metamorphic reactions ceased. Thus, the present garnet rim composition is assumed to reflect diffusional equilibrium adjustment during postculmination retrograde cooling of a particular metamorphic rock.

The calculated steep slopes of the whole rock reactions are consistent with their dehydration nature and water quantity released. The difference in entropy between structurally bound H_2O and H_2O in fluid phase is considerably large and thus the the reaction paths A1 and B1 are quasi vertical (dP / dT = 121 bar/K and 89 bar/K respectively).

These staurolite decomposition reactions and the rock mikrostructure confirm the progressive growth of Grt, Sil in the assemblages (Fig. 2.) and thus form the important feature in the interpretation of the post culmination trajectory. Careful examination of garnet did not prove any important inclusions as they have been homogenised during culmination metamorphic process and existing chemical zonation is clearly related to diffusional processes that have occurred during retrogression. Thus the phase relations of the assemblages examined give reliable constraints on the culmination conditions and retrograde P-T path (Fig. 4.).

Calculated approximative P-T trajectories, in the range of 570-650 °C and 3.5-6.1 Kbar, express the first order tectonic motion and represent specific uplift conditions of the particular tectonic blocks. Some of the samples express uplift trajectories determined dominantly by decompression during cooling while the others may present more isothermal, probably rapid decompression during tectonicaly driven uplift period. The P-T data and the reaction paths are in accordance with index mineral appearances and mineral equilibrium domains. No occurrence of significant retrograde mineral domains and the microscopic appearance of garnets all confirm the individuality of these basement tectonic blocks.

Data for retrograde uplift trajectories (Tab. 3., 4., 5.) indicate an culmination period of higher temperature and medium pressure metamorphic conditions culminating in garnet sillimanite bearing assemblages. These trajectories are consistent with regional metamorphic environment and it is to note that the rock assemblages show differences in P-T conditions attained.

The maximum pressure experienced by the rocks implies that the overburden immediately following the metamorphic culmination stage was of the order of 16 - 20 km. Intrusion of the granodioritic rocks during metamorphic culmination and later might have heated the rocks to different temperatures because of their different ambient geological positions.

It is worth emphasising that not all rock samples collected in the terrane reveal the same P-T histories and confirm exceedingly complex geological development of the area. It is clear from differences in maximum pressures experienced by the rocks that they could not all have been adjacent throughout their metamorphic histories.

Trajectories form loops (Fig.4.) in which the early pressure increase is followed by decrease in pressure at slightly decreasing temperature. Calculated petrogenetic grids (Fig. 6.) determine the sequence of mineral reactions that occured in the studied bulk rock compositins along the assesed P-T path. The calculations in the simplified KMFASH metapelitic system was based on the fluid composition $X_{H2O} = 1$. For calculation of metamorphic culmination fluid composition (X_{H2O}) the equilibrium reaction

Paragonite + Quartz = Albite + Sillimanite + H_2O (4.)

with thermodynamic data of Ferry (1980) and paragonite activity formulation from Eugster et al., (1972) has been used. Thus the composition of metamorphic fluid produced by the reactions A1 and B1 during culmination conditions approaches $X_{H2O} \approx 1$ (see Tab. 7.).

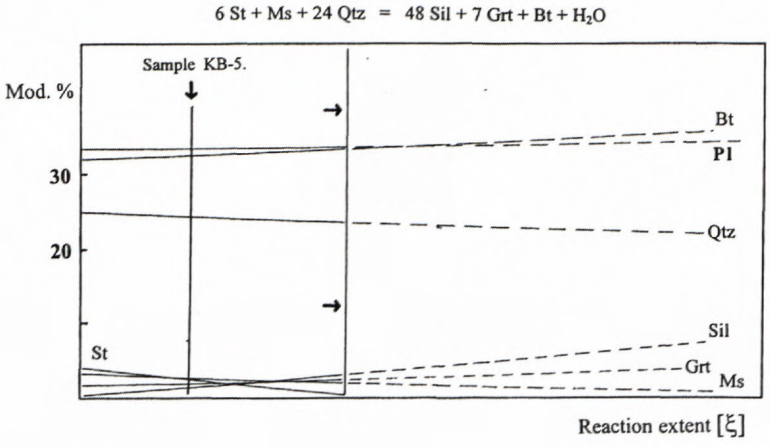

Fig. 3. The calculated changes in the modal proportions of phases with progressive metamorphic reaction path in the low variance assemblage St+Grt+Sil+Bt+Ms+Qtz (sample KB-5). With the reaction progress the proportion of garnet and sillimanite increase at the expense of St + Ms + Qtz. The reaction A1 as presented has not been completed as the consumed reactants (St, Ms) remain present in the assemblage during the expected linear decrease in abundance in sample. As the reaction A1 has the steep slope it is more determined by temperature than by pressure and the implication is that St consumption in observed assemblage has not been completed as the consequence of temperature decrease during cooling and uplift. Later, the proportion of reactants and products remain practically constant and mineral rim compositions have been modified by diffusional processes.

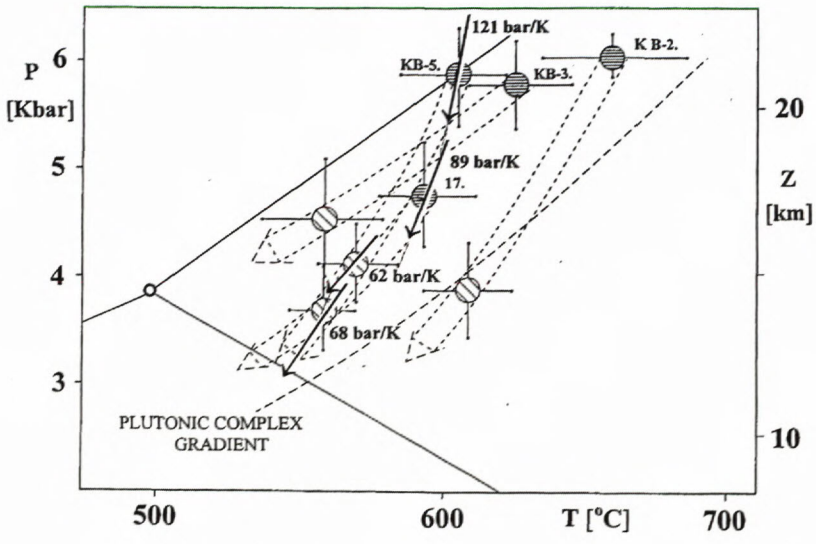

Fig. 4. The calculated metamorphic cumi-nation and closing retrograde P-T charac- teristics of metamorphic recrystallization calculated fromGrt-Bt-Ms-Plg-Sil-Qtz mineral equilibria. The whole rock culmination reaction paths are steep with high dP/dT values (121 bar/K and 89 bar/K for samples KB-5. and 17. Respeti-vely). The post culmination exchange processes near the closing retrograde temperatures have the slopes determined by decompression cooling (see the reactions A2, B2). Temperature data were obtained on the basis of Grt-Bt calibrated equilibria (Ferry & Spear, 1978; Thompson, 1976; Newton & Haselton, 1981; Ganguly & Saxena, 1984; Hodges & Crowley, 1985). Pressure was calculated from calibrated equilibria Grt-Plg-Sil-Qtz (Ghent et al., 1979; Powell & Holland, 1988; Newton & Haselton, 1981) and equilibria including Grt-Bt-Ms-Plg-Qtz (Hoisch, 1990).

The calculated culmination temperatures are considered to produce the equilibrium mineral assemblage with uniform Fe-Mg distribution among the coexisting phases.

The compositional change in the profile of garnet at the biotite-garnet couple interface served as a primary source of data for petrological cooling rate estimates. As the post culmination cooling starts, the equilibrium conditions change with decreasing temperature and drives the diffusion exchange of mobile components at the grain interface boundaries. The diffusion process continue till the retrograde closure temperature froze in the compositional changes in garnet realised during cooling. The diffusion garnet profiles were then normalised for Mg concentrations as a function of normalised distance from the Bt-Grt edge to obtain the shape of the garnet compositional profile. Diffusion formalism and equations of Lasaga et al., (1977) and Lasaga (1983) served as the methodical tool and computation basis for petrological cooling rates estimates (Tab. 8.). However, for reliable and consisting cooling rate approximation more than 3-5 garnet compositional profiles have to be studied in a sample and more accuratete activation energy (ΔE*) data are needed for calculation of accurate petrological cooling rate data for the paragneisses of the studied geological area.

Discussion

Most of the mountain belts of the world are believed to be the result of continental collision (Bird & Dewey, 1970). The first thermal model of continental collision was published by Oxburgh & Turcotte (1974) with respect to the Tauern Window in the Eastern Alps. Its metamorphic P-T evolution inferred from thermobarometry and fluid inclusions has been calculated by Selversone et al., (1984), Selverstone (1985), Selverstone & Spear (1985), Spear & Franz (1986).

The retrograde P-T path is easier to obtain than the prograde path and thus most is known about the cooling histories of concrete terranes. However, in order to distinguish between different tectonic scenarios more information on the prograde portion of the path is required. Then the P-T path can place constraints on the depth and thermal conditions during fault movement or may even provide clues as to the existence of a fault where field evidence is ambiguous.

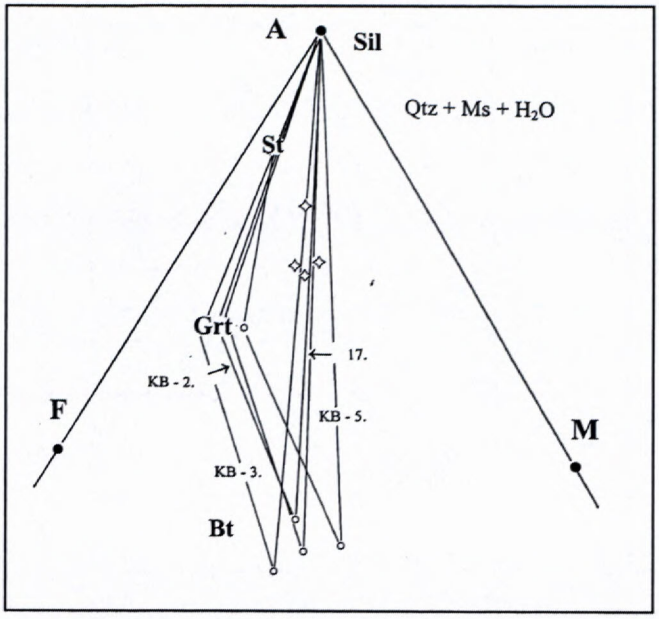

Fig. 5. Schematic AFM diagram representing studied mineral compositions and compatibility of phase relations. The bulk rock compositions (✧) are also presented. The sequence of the mineral assemblages depends on P-T trajectory and chemical composition of rock. Staurolite decomposition St → Sil + Grt + Bt in the studied assemblages (including Qtz + Ms + H_2O) is consistent with the whole rock reaction path and the mass balance of coexisting AFM minerals in rocks (see reaction A1, B1). Thus sillimanite appears, staurolite is consumed, and kyanite may eventually disappear during the reaction changes. The stability field of cordierite at calculated P-T conditions has been ignored. Formulas of Thompson (1957) have been used for the calculating and plotting the positions of minerals on the diagram: A=Al_2O_3-3K_2O, F=FeO, M=MgO.

The Alpine type P-T path is characterized by nearly isothermal decompression, which can only be caused by rapid exhumation and is generally thought to be cauased by either tectonic unroofing such as occurs in the extensional terranes or by very rapid erosion (Ernst, 1973, 1988). Ernst cit. attributes the cause of rapid exhumation to the shift from the subduction of crust to the collision. Tectonic changes caused by continental collision result in rapid uplift of the higher pressure rocks and denudation by erosion or tectonically. The thermal relaxation may cause only minor heating that is frequently followed by rock cooling. The extension dynamics allows the underplated rocks to rise eventually to the earth surface where they are currently exposed. The time scale for the exhumation of higher graded metamorphic rocks is on the order of 10 - 15 Ma (Ernst, 1988).

Isothermal decompression paths are most likely produced by tectonic thickening of the crust followed by exhumation dominated by either erosion or tectonic denudation (England & Richardson, 1977; England & Thompson, 1984). Tectonic denudation will produce a steeper decompression path than erosion alone and Anovitz & Chase (1990) argue that some type of tectonic denudation is required to explain the shapes of isothermal decompression P-T paths.

Isobaric cooling paths (IBC) are more difficult to interpret unless some portion of the prograde P-T path can be deduced. IBC paths may arise from counterclockwise P-T loops as has been suggested by Bohlen (1987). In this interpretation the heat source for the early low pressure, high temperature part of the path is assumed to be magma accreation beneath existing crust.

Magma accreation at the base of the crust will produce an elevated geotherm and subsequent thermal relaxation will cause a long period of isobaric cooling. Continual thickening and rapid exhumation may give rise to isothermal decompression paths for rocks of the upper crustal block.

P-T characteristics of culmination recrystallisation of the M.K. basement paragneisses have been determined earlier (Dyda, 1977, 1980a,b; Pertchuk et al., 1984; Dyda and Miklóš, 1993).

Korikovskii et al., 1984 present for the whole M.K. metamorphic region the pre culmination trend as isobaric heating recrystallisation process characterized by pressures ca. 3.3 Kbar and temperatures extent of ca. 350-550 °C. These trends are fully accepted by Krist et al., (1992). Thus the isobaric heating presupposed by these authors runs in progressive pre culmination metamorphic stages in the And stability field and the P-T trends would be typical of contact metamorphic terrane where crust has had considerable heat added by the addition of magmas. Isobaric heating might have been confirmed by garnet zonality development, reaction sequences and reaction slopes in equilibrium assemblages. Anyhow, the crucial contact metamorphic assemblages with And + Crd are missing in the Bratislava massive area studied by the author. Thus, the paths might have started out at similar conditions and end at nearly the same temperature, but followed different trajectories in essentially different metamorphic thermal regime.

The metamorphic trajectories, presented here, represent "clockwise" post culmination decompression cooling (Fig. 4.), that is typical of regions that have undergone crustal thickening followed by thermal relaxation and are principally different from isobaric heating trajectories. The early part of the trajectory is a heating phase through the kyanite stability field and is interpreted to result from regional metamorphism. The pressure peak was followed by slightly heating period and decompression cooling. As there is no reheating or significant retrogression signs the major Variscan orogeny is believed to have been caused by collision of the continental fragments. The differences in peak temperatures, pressures and cooling might show approximate position of the units along P-T at various stages of convergence followed by thermal relaxation and are not considered to represent some major fundamental differences in the tectonic setting.

A significant difference between low pressure parageneisses and studied intermediate pressure parageneses is that at low pressures, the composition of minerals are closer to the Fe-end members in the KMFASH system and increasing temperature results in the assemblage with andalusite + cordierite. If the sillimanite precursor in low pressure

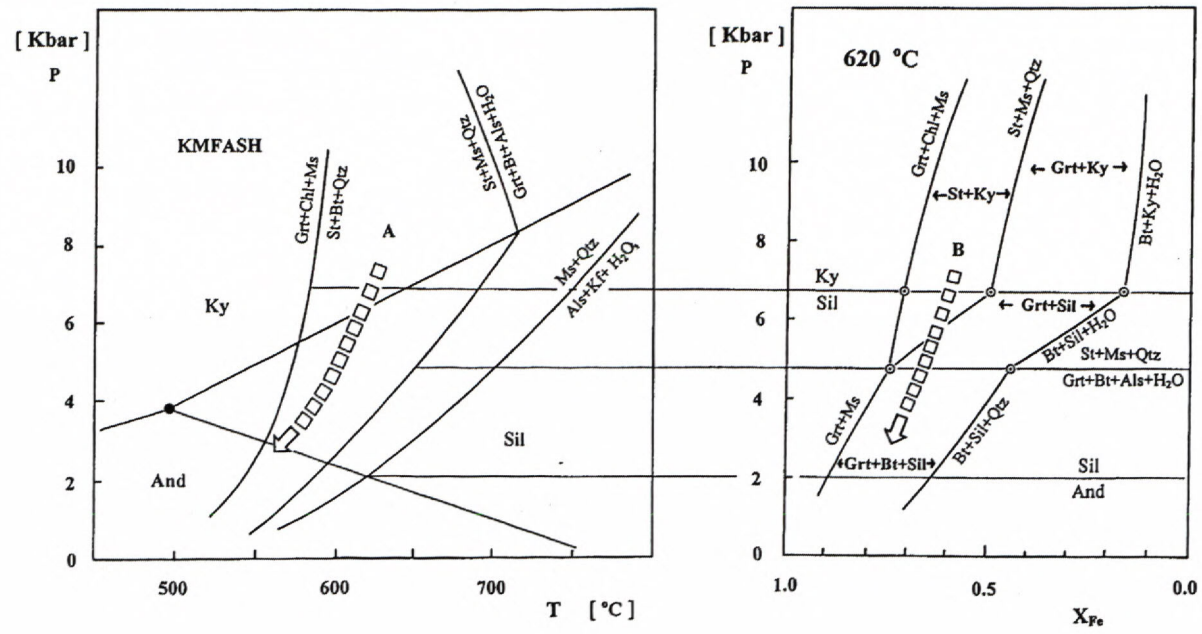

Fig. 6. Isothermal pseudobinary P-X_{Fe} section at culmination temperatures (~ 620 °C) presenting divariant reaction fields and phase relations among St-Grt-Sil-Bt-Ms-Qtz-H_2O in the simplified matapelitic KMFASH model system. X_{Fe} for the studied rocks is taken from the Tab. 1., X_{H2O} is taken to be 1 (see Tab. 7.). Path A is the generalised decompression trajectory during cooling of the crystalline complex obtained on the basis of the geothermobarometric data and the higher pressure kyanite rests present. Path B expresses decompression intersection of the reaction boundary St+Ms+Qtz = Sil+Grt+Bt+H_2O consistent with the microscopic texture and the whole rock reaction path based on the thermal culmination mass balance.

Table 7. Fugacity (f, bars) and the mole fraction of water (X_{H2O}) in metamorphic fluid at the culmination conditions calculated from the equilibrium Par + Qtz = Ab + Sil + H_2O.*

Sample	X_{Ab}	X_{Pa}	γ_{Pa}	fH_2O	X_{H2O}
17.	0.787	0.286	3.797	2309	0.96
KB-5.	0.755	0.196	4.789	3734	0.98

*Thermodynamic formulation of the reaction is according to Ferry (1980): $\Delta H°_R$ = 91190 J, $\Delta S°_R$ = 169.12 J K^{-1}, ΔV_S = - 0.447 J bar^{-1}. X_{Ab} - mole fraction of albite in plagioclase; γ_{Pa} - activity coefficient for paragonite.

Table 8. Petrological cooling rate estimates for Malé Karpaty Tatric basement paragneisses.

Sample	17.	KB-2.	KB-3.	KB-5.
T [°C]	592±17	657±25	623±21	601±19
P [Kbar]	4.66±0.45	5.90±0.05	5.70±0.41	5.82±0.41
r [mm]	0.604	0.366	0.384	0.359
Diffusion coefficient [cm^2/s] *				
D_T(Ch&G)	$9.99*10^{-21}$	$1.48*10^{-19}$	$3.87*10^{-20}$	$1.55*10^{-20}$
D_T(F)	$1.00*10^{-20}$	$2.84*10^{-19}$	$5.24*10^{-20}$	$1.64*10^{-20}$
D_T(E)	$2.30*10^{-19}$	$2.04*10^{-18}$	$6.78*10^{-19}$	$3.18*10^{-19}$
D_T(L)	$5.49*10^{-20}$	$9.48*10^{-19}$	$2.55*10^{-19}$	$8.35*10^{-20}$
γ'	279	24	33	26
Cooling rate [°C/Ma]				
S (Ch&G)**	4.07	1.86	2.66	0.22
S (F)	4.01	3.56	3.61	0.24
S (E)	94.03	25.62	46.71	4.69
S (L)	22.39	11.89	15.48	1.23

* calculated for metamorphic culmination P-T conditions using pre-exponential factor D_0 and activation energy for diffusion Δ E* according to **Ch&G - Chakraborty & Ganguly (1992), F - Freer (1981), E - Elphic et al., (1985), L - Lasaga (1977). Cooling rate [*S*] has been calculated according to formula of Lasaga (1983), $S = RT^2 \gamma'/\Delta E^* a^2$. γ'- is given by the shape of the measured composition profile and *a* is the garnet size.

mineral assemblages was andalusite ± cordierite, the recrystallisation obviously produces crystals of sillimanite and corresponding mineral changes over ca. 550 °C lead to stable, final peak low pressure contact metapelitic assemblage Sil+Crd+Bt+Ms±Grt+Qtz. Sillimanite present in the studied samples has, however, the appearance of fibrolitic form that is frequently, typically encountered on the regional metamorphic trajectories where mineral transformations kyanite → sillimanite occur.

Although there is some scatter in the studied P-T paths, most of the paths show simultaneous decompression and cooling, consistent with the P-T data, whole rock reaction paths their slopes and the reaction sequence.

The regional cooling and exhumation processes depend on the trajectory shape expressing the tectonometamorphic evolution recorded by reaction paths and geothermobarometry. The regional metamorphism in the area has been documented (Dyda, 1997) by slow rate of nucleation $2.9*10^{-8}$ cm^3/s - $1.0*10^{-7}$ cm^3/s, the reaction temperature overstep of ca. 0.15 °C/y and the modeled progressive heating rate trends of $4*10^{-5}$ °C/y, they are in good agreement with the characteristics of the regional metamorphic thermal regime (see e.g. Thompson & England, 1984 for comparison).

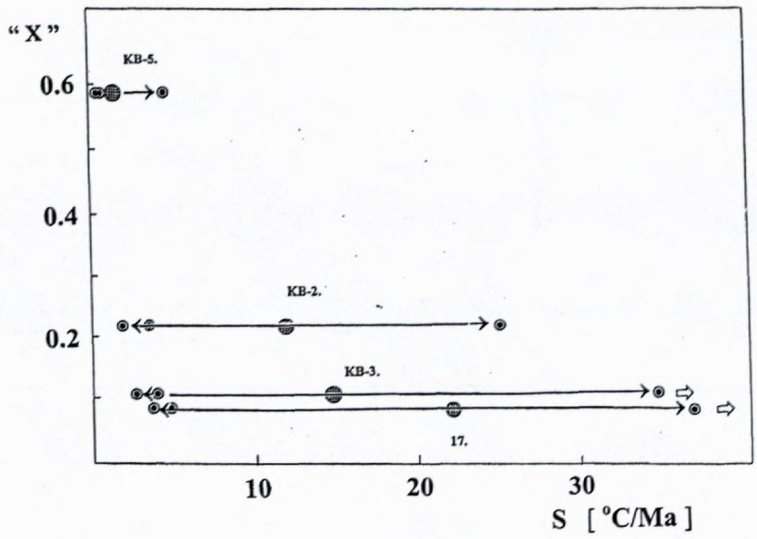

Fig. 7. The calculated cooling rate (S, °C/Ma) and the extent of garnet mass transfer ("X") in the mineral assemblages of basement paragneisses express the mutual relation between these petrological characteristics when rapid cooling enables only limited mass transfer and lasted residence of rock at higher postculmination temperatures favours assemblage ripening and diffusion adjustment processes.

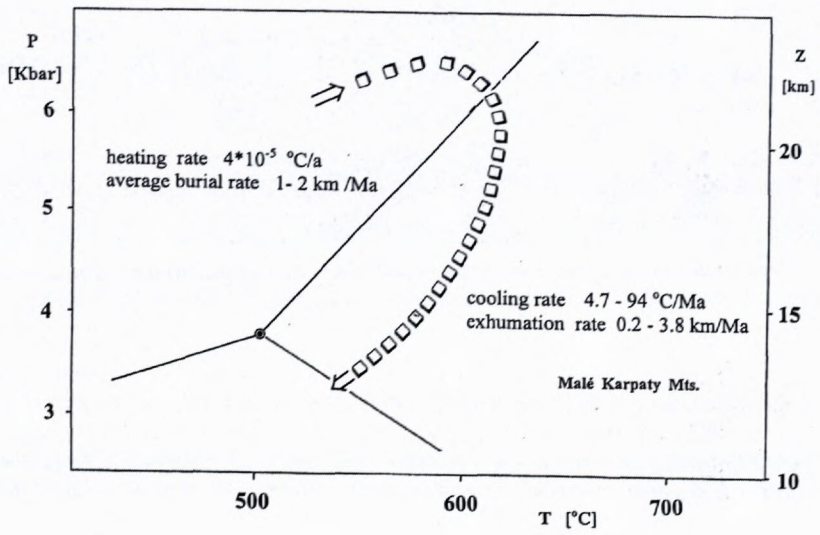

*Fig. 8. Approximative time characteristics for Bratislava massive Tatric basement metamorphic trajectories inferred from petrological data. Average heating rate of the regional metamorphic complex (4*10^{-5} °C/a) was determined on the basis of garnet crystal size distribution and is consistent muscovite dehydration time (unpib-lished data). In linear approximation, after anchimetamorphic zone crossing (ca. 150-200 °C) time of ca. 11 Ma is needed for metamorphic complex to reach thermal culmination ~600 °C in depth of ~24 km. In this numerical approximation, average bu- rial rate ~ 1-2 km may be considered. The cooling rates calculated on the basis of diffusional zoning in garnets and Elphic et al., (1985) experimental data are in the range of 4.7- 94 °C/Ma. The exhumation rate of the Tatric basement complex is then consequently ca. 0.2 - 3.8 km/Ma.*

The regional recrystallisation products are usually subjected to prolonged cooling after thermal culmination ceased and processes of the assemblage ripening and diffusion adjustment operate. The diffusion processes and the annealing mass transfer are temperature and time dependent mineral changes. The calculated values of the post culmination garnet mass transfer (X = 0.10-0.53) are in particular samples significantly different documenting different annealing processes that lasted after the thermal culmination was attained and completed (Dyda, 1997).

Morphological appearance of idioblastic garnets with steep, narrow retrograde diffusion rims clearly testify rapid cooling during uplift. The apparently quenched mineral assemblages of particular tectonic blocks differ from the other assemblages which exhibit significantly higher garnet mass transfer estimates and different cooling history.

The tectonic reconstruction may partially use the estimates of crustal overburden that is inferred from computed changes in pressure. When these P-T data are combined with other petrological inferences including post culmination garnet mass transfer and aproximated petrological cooling rates (Fig. 7.), the observed P-T paths can then be useful for constraining tectonic differences in transport rates as well as of exhumation.

The duration of metamorphic event may be considerably long, estimates are well in excess of 100 Ma inferred on the basis of cooling rates of 1 °C/Ma. As many minerals crystallize at prograde, others at culmination temperature and some at retrograde stages, the determination of equilibrium in particular thin sections may be complicated. Certain minerals have refractory nature and do not equilibrate easily during cooling (Sharp and Ulmer, 1993) and peak conditions may be assessed in carefully selected rocks.

In first numerical approximation, the petrological subduction estimates have been based on calculated peak temperature, depth and heating rate data (4*10^{-5} °C/a) that provide corresponding average burial rate value of 1-2 km/Ma for the studied basment paragneisses (Fig. 8.). The petrological cooling rate data obtained on the basis of evaluation of the diffusional zonality development in gar-

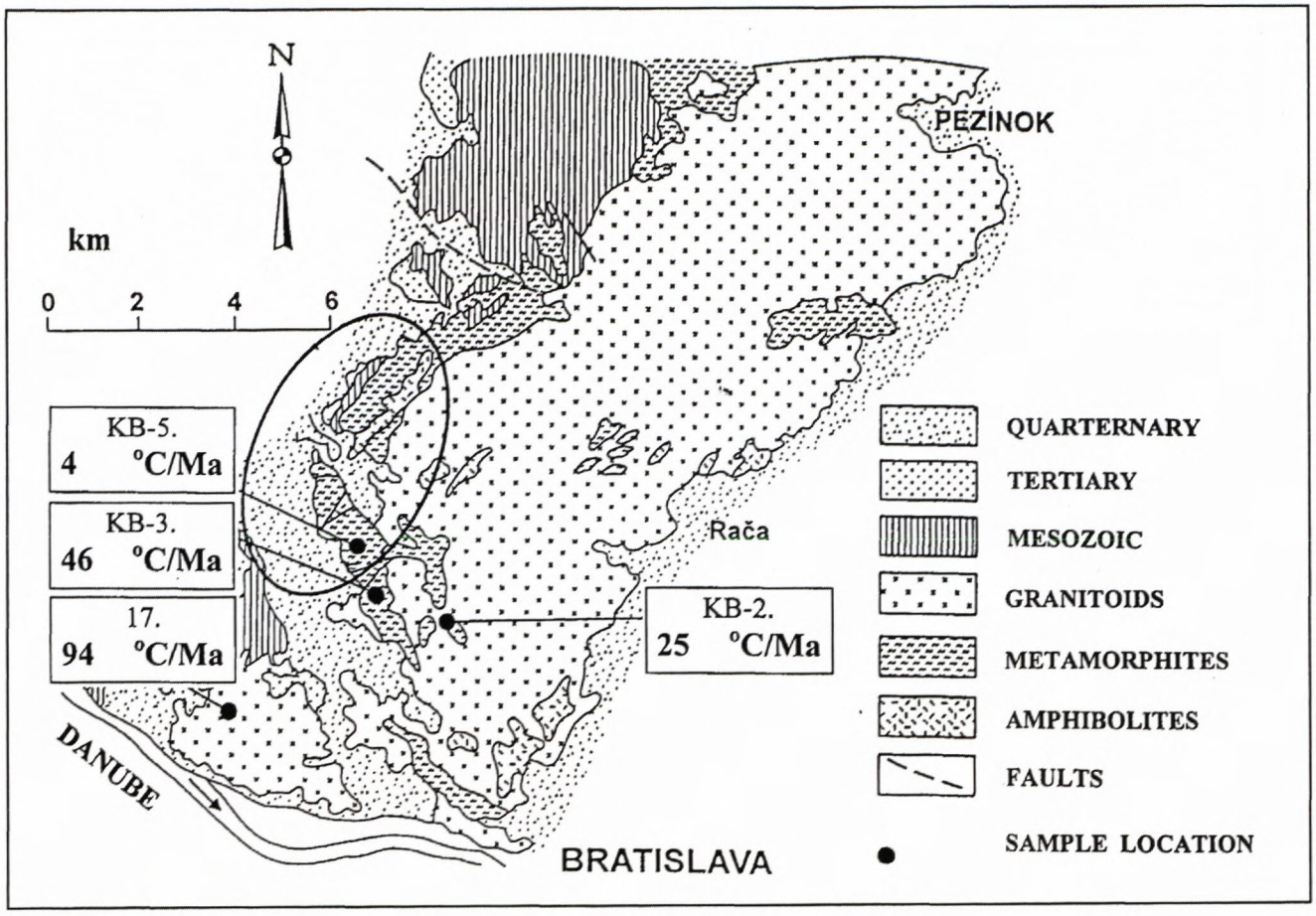

Fig. 9. Petrological cooling rate estimates S (°C/Ma) for the Tatric basement paragneisses present considerable differences. This scattering is petrologically confirmed by differences in post culmination garnet mass transfer when quenched metamorphic assemblages exhibit minimum transfer changes. The S data are considered to represent the individuality of post culmination cooling development and fragmentation of the Tatric basement into Variscan tectonic blocks. For cooling rate calculation the diffusional parameter D_0 and activation energy for garnet diffusion ΔE^* have the crucial importance. However, more unifying, reliable diffusional characteristics are still missing and thus for cooling rates comparison the calculated S values of Elphic et al., (1985) are shown as they probably represent the most realistic cooling rate scenario in the Malé Karpaty Variscan basement. The geological area circled has been earlier subjected to the *detailed periplutonic author's studies.*

nets (Tab. 8.) may assess the approximate exumation rate at 0.2 - 3.8 km/Ma for the Tatric metapelitic basement rocks.

Different diffusion zonality development and calculated post culmination cooling rates clearly document that the basement rocks stayed different period of time under thermal culmination conditions. The data presented (Tab. 8, Fig. 8, Fig. 9) form thus the first comparison basis for petrological heating and cooling rates in the Western Carpatian region.

The scattering of "*S* "data is partly caused by accepting cited D_o and ΔE^* of different authors. This lead after computation consequently to scattered diffusion coefficients and cooling rates estimates.

From Spanish Betic metamorphic terranes minimum cooling rates of 200 °C/Ma are reported and uplift rates of 2 - 5 km/Ma have been given (Zeck et al., 1989). For the same geological area Monié et al., (1994) report cooling rates of 150-350 °C/Ma and corresponding exhumation rates of 5-10 km/Ma. For Tauern Window the exhumation rate varied from >5 km Ma to < 1 km/Ma (Clif et al., 1985). Exhumation and cooling rate of Dora Maira terrane are 22 km/Ma and ca. 90 °C/Ma respectively (Gebauer, 1996).

Detailed cooling rate data for Buckskin-Rawhide metamorphic core complex (Scott et al., 1998) however reveal non-linear cooling process, as cooling rate of these rocks increased progressively, peaking at 280 °C/Ma documenting tectonically driven abrupt increase in cooling rates. This implies that cooling did not keep pace with denudation at upper crustal levels where high cooling rates primarily reflect the development of thermal diccontinuity accros the detachment fault.

The above methodical approach illustrates the types of different petrologic information that may be utilized in deciphering the evaluation of complex metamorphic terranes and their tectonic development.

Conclusions

The Variscan regional metamorphic processes in Malé Karpaty Tatric basement rocks attained conditions of amphibolite facies with temperatures of ~ 570–620 °C

(Tab.3.) and pressure span ~ 4.5-6.1 Kbar (Tab. 4,5.). The culmination conditions in particular tectonic blocks represent different P-T data, metamorphic reaction extent and postculmination uplift characteristics expressed by mass transfer, diffusion zonality development and different cooling rates of particular rock blocks.

The culmination mineral assemblages (Tab.1.), index mineral appearance, sequence and extent of discontinuous metamorphic reactions (Fig.3.) and metamorphic fluid composition (Tab.7.) are consistent with the metapelitic KMFASH model system (Fig. 5, Fig. 6.) and the calculated geothermobarometric data.

The culmination temperatures, pressures, whole rock reaction reaction paths and uplift trajectories of particular crystalline blocks (Fig. 4.) represent complex differences of Variscan tectonothermal activity in the Variscan basement. The crustal level conditions of intrusive magmatism may be approximated by 16 - 20 km for most granitoidic intrusions of Bratislava massive. The peak metamorphism is probably associated with the polyphase granitoid intrusions and thus some sillimanite bearing assemblages may be synchronous with plutonism in the area. However, to built an reliable detailed orogenic model, more data controlling the crustal heat distribution, tectonics and postculmination cooling are needed.

The whole rock metamorphic culmination reactions (Tab.6.) have steep, quasi vertical slopes ($dP/dT \approx 89$-121 bar/K) determining almost isothermal decompression as a consequence of rapid tectonic uplift and erosion. Post culmination cooling processes associated with diffusional equilibrium adjustment was characterized by decompression cooling with the slopes $dP/dT \approx 62$-68 bar/K. Cooling rates of the rock blocks were different ($S \approx 4.7$-94 °C/Ma, Tab. 8, Fig. 9) and express first order tectonic fragmentation of Tatric basement rocks during Variscan crustal collision and shortening. Although there is some scatter in the P-T paths they show simultaneous decompression and cooling. Orogenic specific exhumation conditions and cooling rates data characterize rapid tectonic processes in the basement rocks at the collisional Variscan orogenic wedge.

However, the determined regional 'clockwise' metamorphic trajectories for particular paragneisses in the Bratislava granitoidic massive area, based on thermobarometry, reaction extent, reaction slopes and kyanite appearence, differ substantially from Crd+Sil assemblages in periplutonic zones of Modra massive described by Korikovkij et al., (1984) as a result of periplutonic isobaric heating.

The multiple heating events are absent and the studied metamorphic rocks display the mineral assemblage and mineral chemical composition reflecting the culmination metamorphic temperatures and later diffusional equilibrium mineral adjustment. Metamorphic grade increased to the peak metamorphic assemblages post-dating and eradicating earlier metamorphic assemblages and fabrics and thus the culmination mineral assemblage document single Variscan metamorphic event with different intensity of post culmination retrograde changes on the scale of metamorphic crystalline core. The Alpine tectono deformation processes destroyed and displaced the crystalline basement units and emplaced previously assembled complexes into new tectonic structural positions.

The differences in peak temperatures, pressures and cooling rates predict discontinuities in P and T in crustal depths and are considered to form an additional evidence that the post metamorphic faulting juxtaposed the rock blocks of different P-T characteristics and the fragmented basement area was a locus of major tectonic fault.

Acknowledgements

Thanks are expressed to Dr.F.Caňo, Doc.Dr.J.Krištín form Faculty of Science, Comenius Univeristy, for microprobe analytical work. Special thanks are due to W. Edwards (Kingston University, England) for kindly realized garnet analyses.

References

Andrusov, D. 1936: Subtatric nappes in Western Carpathians. Carpathica, Praha, 1, 5-50.

Andrusov, D. 1968: *Grundriss der Tektonik der Nördlichen Karpaten.* Veda SAV, Bratislava, 188 p.

Andrusov, D., Bystrický, J. & Fusán, O. 1973: *Outline of the Structure of the West carpathian.* Guidebook for Geological Excursions. GÚDŠ, Bratislava.

Anovitz, L. M. & Chase, C. G. 1990: Implications of post-thrusting extension and underplating for P-T-t paths in granulite terranes. A Grenville example.Geology,18, 466 - 469.

Bird, J. M. & Dewey, J. F. 1970: Litghospheric plate - continental margin tectonics and the evolution of the Appalachian orogen. Geol. Soc. Amer. Bull., 81, 1031 - 1060.

Bagdasarjan, G.P., Gukasjan, R.Ch., Cambel, B. & Veselský, J. 1983: Resuľtaty Sb-Sr opredeleniji vozrasta metamorfičeskich porod kristaličeskogo komplexa Malých Karpat. Geol.Zborn.Geol. Carpath., 34, 4, 387-397. (in Russian).

Bezák, V. 1993: Herýnska a alpínska tektogenéza západnej časti Slovenského rudohoria: základné štádiá vývoja. In *Geodynamický model a hlbinná stavba Západných Karpát.* Rakús, M. &- Vozár, J. Eds.,.Geologický ústav Dionýza Štúra, Bratislava 1993., 243 - 247. (in Slovak, Engl. summary).

Bezák, V., Jacko, S., Ledru, P. & Siman, P. 1998: Hercynian development of the Western Carpatihans. p.27-34. 45. In: Rakús, M. ed., 1998: *Geodynamic development of the Western Carpathians.* Dionýz Štúr Publishers, Bratislava, 290 p.

Bohlen, S. R. 1987: Pressure - temperature - time path and a tectonic model for the evolution of granulites. J. Geology, 95, 617 - 632.

Broska, I. & Janák, M. 1985: Akcesorické minerály metapelitov a ich vzťah k metamorfóze v oblasti Záhorskej Bystrice (Malé Karpaty). In: *Akcesorické Minerály ich Petrogenetický a Metalogenetický Význam.* GÚDŠ Bratislava, 101-106. (in Slovak, Engl. summary)

Cambel, B. 1952: Amfibolické horniny v Malých Karpatoch. Geol. Práce, Zoš., 29, 70 (in Slovak).

Cambel, B. 1954: K otázke kryštalických bridlíc medzi Cajlou a Hornými Orešanmi v Malých Karpatoch. Geol. Práce, Spr., 1, 16-20. (in Slovak).

Cambel, B. & Valach, J. 1956: Granitoidné horniny v Malých Karpatoch, ich geológia, petrografia a petrochémia. Geol. Práce, Zoš., 42, 113-268.(in Slovak, Engl. summary).

Cambel, B. & Vilinovič, V. 1987: *Geochémia a petrológia grantoidných hornín Malých Karpát. Veda, Vyd. SAV, Bratislava, 183 p.* (in Slovak, Engl. summary).

Cambel, B., Dyda,M. & Spišiak,J. 1981: Thermodynamic measurement of origin of minerals in the area of crystalline of Malé Karpaty Mts., Geol. Zbor. Geol. Carpath., 32, 745 - 768.

Cambel, B., Miklóš, J., Khun, M. & Veselský, J. 1990a: Geochémia a petrológia ílovito-kremitých metamorfovaných hornín kryštalinika Malých Karpát. *ŠVK,* Banská Bystrica, 267 p. (in Slovak, Engl. summary).

Cambel, B., Kráľ, J. & Burchart, J. 1990b: Izotopová geochronológia kryštalinika Západných Karpát. *Veda, Vyd. SAV,* Bratislava, 183 p. (In Slovak, Engl. summary).

Cliff, R.A., Droop, G.T.R, & Rex, D.C. 1985: Alpine metamorphism in the south-east Tauern Window, Austria. 2.Rates of heating, cooling and uplift. J.Metamorphic Geol., 3, 403-415.

Crowley, P. D. 1991: Thermal and kinetic constraints on the tectonic applications of thermometry. Mineral. Mag., 55, 57 - 69.

Dyda, M. 1977: Indexové minerály pararúl v oblasti bratislavského granitoidného masívu. *Disertation.* Manuscript - GÚ SAV, Bratislava, 136 p.(in Slovak).

Dyda, M. 1980a: Physical properties and temperatures of crystallization of coexisting garnets and biotites from paragneisses of the Little Carpathians. Geol. Zbor.Geol. Carpath., 31, 201- 213.

Dyda, M. 1980b: Metamorphic grade and packing index in garnets. Geol. Zborn. Geol. Carpath., 31, 359 - 374.

Dyda, M. 1994: Geothermobarometric characteristics of some Tatric crystalline basement units (Western Carpathians). Mitt. Österr. Geol. Ges., 86, 45 - 59.

Dyda, M. 1997: Disturbance of the Variscan metamorphic complex indicated by mineral reactions, P-T data and crystal size of garnets (Malé Karpaty Mts.). In: Grecula, P. Hovorka, D. & Putiš, M. edts. 1997: *The Geological Development of the Western Carpathians,* Mineralia Slovaca Monographs, Bratislava.

Dyda, M. 1999: Fragmentácia metamorfného obalu bratislavského masívu indikovaná vlastnosťami granátov. Mineralia Slov., 31, 39 - 48.(in Slovak, Engl. summary).

Dyda, M. 2000: Exhumation and cooling rates of the Variscan basement metamorphic complex inferred from petrological data (Malé Karpaty Mts.), Slovak Geol..Mag., 6, 2-3, 293 - 297.

Dyda, M. & Miklóš, J., 1993: Periplutonické zóny bratislavského granitoidného masívu (Malé Karpaty): rekryštalizácia, dehydratačné a objemové zmeny. Mineralia Slov., 25, 93 - 103.(in Slovak, Engl. summary).

Elphick, S.C., Ganguly, J. & Loomis, T.P. 1985: Experimental determination of cation diffusivities in aluminosilicate garnets. I. Experimental methods and interdiffusion data. Contrib.Miner.Petrol., 90, 36-44.

England, P. C. & Richardson, S. W. 1977: The influence of erosion upon the mineral facies of rocks from different metamorphic environments. J. Geol. Soc. London, 134, 201 - 213.

England, P.C. & Thompson, A.B. 1984: Pressure-temperature-time paths of regional metamorphism. I.-Heat transfer during the evolution of regions of thickened continental crust. J. Petrology, 25, 894-928.

Ernst, W.G. 1973: Interpretive synthesis of metamorphism in the Alps. Geol. Soc. Am. Bull., 84, 2053-2078.

Ernst, W.G. 1988: Tectonic history of subduction zones inferred from retrograde blueschist P-T paths. Geology, 16, 1081-1084.

Eugster, H.P., Albee, A.A., Bence, A.E. & Thompson, J.B.Jr. 1972: The two-phase region and excess mixing properties of paragonite-muscovite crystalline solutions. J. Petrology, 13, 147-179.

Ferry, J.M. 1980: A comparative study of geothermometers and geobarometers in pelitic schist from south-central Maine. Amer. Mineralogist, 64, 720-732.

Ferry, J.M. & Spear, F.S. 197: Experimental calibration of the partitioning of Mg and Fe between biotite and garnet. Contrib. Mineral. Petrology, 66, 113 - 117.

Ganguly, J. & Saxena, S.K. 1984: Mixing properties of alunimosilicate garnets: constrains from natural and experimental data and applications to geothermobarometry. Amer. Mineralogist, 69, 88 - 97.

Gebauer, D. 1996: A P-T-t path for (ultra?-) high-pressure ultramafic/mafic rok associations and their felsic country rocks based on SHRIMP dating of magmatic and metamorphic zircon domains: example: Alpe Arami (Central Swiss Alps). In: Basu, A., Hart, S., eds. Earth Processes: reading the isotopic code.Geophys Monograph Series, 95, 307-329.

Ghent, E. D., Robbins, D. B. & Stout, Z.M. 197: Geothermometry, geobarometry and fluid composition of metamorphosed calc-silicates and pelites, Mica Creek, British Columbia. Amer. Mineralogist, 64, 874 - 885.

Ghent, E. D. & Stout, Z.M. 1981: Geobarometry and geothermometry of plagioclase-biotite- garnet-muscovite assemblages. Contrib. Miner. Petrol., 76, 92-97.

Hodges, K. V. & Crowley, P. D. 1985: Errror estimation in empirical geothermobarometry for pelitic systems. Amer. Mineralogist, 70, 702 - 709.

Hoisch, T. D. 1990: Empirical calibration of six geobarometers for the mineral assemblage quartz + biotite + plagioclase + garnet. Contrib. Mineral. Petrology, 104, 225 - 234.

Holland, T.J.B. & Powell, R., 1998: An internally consistent thermodynamic data set for phases of petrological interest. J. Metamorphic Geol., 16, 309 - 343.

Korikovskij, S.P., Cambel, B., Miklóš, J. & Janák, M. 1984: Metamorphism kristallinikuma Malych Karpat. Zonalnosč, etapy, svjiaz s granitoidami. Geol. Zborn. Geol. Carpath., 35, 437 - 462.

Koziol, A. M. & Newton, R. C. 1988: Redetermination of the anorthite breakdown reaction and improvement of the plagioclase-garnet-Al2SiO5-quartz geobarometer. Amer. Mineralogist, 73, 216-223.

Krist, E., Korikovskij, S.P., Putiš, M., Janák, M. & Faryad, S.W. 1992 : *Geology and Petrology of Metamorphic Rocks of the Western Carpathian Crystalline Complexes.* Comenius University Press, Bratislava 1992, 324 s.

Lasaga, A.C. 1983: Geospeedometry: an extension of geothermobarometry. In: Saxena, S. K., (ed.) *Kinetics and Equilibrium in Mineral Reactions.* Advances in Physical Geochemistry 3., 81-114.

Lasaga, A.C., Richardson, S.M. & Holland, H.D. 1977: The mathematics of cation diffusion and exchange between silicate minerals during retrograde metamorphism. In: Energetics of Geological Processes (ed. Saxena, S.K. & Battachanji, S.), s. 353-388. Springer Verlag, New York.

Leško, B., Beránek, B.& Varga, I. 1980: Cisailements horizontaux profonds sous les Karpates occidentales a la lumiere des connaissanses géophysiques. Rev. Géol. dyn. Géogr. phys., 22, 255-266.

Lugeon, M. 1903: Les nappes de recouvrement de la Tatra et l´origine des Klippes des Carpathes. Bull.Lab.geol.Univ., Lausanne, 4.

Maheľ, M. 1983: Beziehung Westenkarpaten-Ostalpen, Position des Ubergangs - Abschnittes, Deviner Karpaten. Geol. Zborn. Geol. Carpath., 34, 131 - 149.

Maheľ, M. 1986: Geological Structure of the Czechoslovak Carpathians. Paleoalpine Units I. Veda SAV, Bratislava.

Marko, F., Fodor, L. & Kováč, M. 1991: Miocene strike-slip faulting and block rotation in Brezové Karpaty Mts. (Western Carpathians). Mineralia Slov., 23, 189 - 200.

Miklóš, J. 1986: Petrológia kryštalických bridlíc metamorfných zón Malých Karpát. Mineralia Slov., 18, 179 - 180.

Miklóš, J. 1987: Príspevok k štúdiu protolitu kryštalických metamorfných zón Malých Karpát. In: *Sborník príspevku z II. Celostátní konference mineralogu a petrologu.* Brno-Blansko, 93 - 95.

Monié, P., Torres-Roldan, R.L. & Garcia-Casco, A. 1994: Cooling and exhumation of the Western Betic Cordilleras, 40Ar/39Ar thermochronological constraints on a collapsed terrane. Tectonophysics, 238, 353-379.

Newton, R. C. & Haselton, H. T.: Thermodynamics of the garnet - plagioclase - Al_2SiO_5 - quartz geobarometer. In: Newton, R.C., Navrotsky, A., & Wood, B.J. (Eds.): *Thermodynamics of minerals and melts,* 131 - 147, Springer Verlag, New York.

Oxburgh, E. R. & Turcotte, D. L. 1974: Thermal gradients and regional metamorphism in overthrust terrains with special reference to the eastern Alps. Schweiz. Mineral. Ptrol. Mitt., 54, 641 - 662.

Pertchuk, L. L., Lavrentieva, I. V., Kotelnikov, A.R. & Petrík, I. 1984: Comparison characteristics of thermodynamic regimes of the Maine Caucazus chain and West Carpathians (in Russian), Geol.Zborn.Geol.Carpath., 35, 105-156.

Plašienka, D. 1989: Štruktúrny vývoj tatrika Malých Karpát. Mineralia Slov., 21, 538.

Plašienka, D., Michalík, J., Kováč, M., Gross, P. & Putiš, M. 1991: Paleotectonic evolution of the Malé Karpaty Mts. - An overview. Geol. Carpath., 42, 195 - 208.

Powell, R. & Holland, T.J.B. 1988: An internally consistent dataset with uncertainties and correlations: 3.Application to geobarometry, worked examples and computer program. J. Metamorphic Geol., 6, 173 - 204.

Putiš, M. 1987: Geológia a tektonika juhozápadnej a severnej časti kryštalinika Malých Karpát. Mineralia Slov., 19, 135-157. (in Slovak, Engl. summary).

Putiš, M. 1991: Tectonic styles and Late Variscan-Alpine evolution of the Tatric - Veporic crystalline basement in the Western Carpathians. Zbl. Geol.Paleont. Teil.l, H.1, 181 - 204.

Scott, R. J., Foster, D. A. & Lister, G. 1998: Tectonic implications of rapid cooling of lower plate rocks from the Buckskin-Rawhide metamorphic core complex, west-central Arizona. Geol. Soc. Amer. Bull., 110, 588 - 614.

Selverstone, J. 1985: Petrologic constraints on imbrication, metamorphism and uplift in the SW Tauern Window, Eastern Alps. Tectonics, 4, 687-704.

Selverstone, J. & Spear, F. S. 1985: Metamorphic P-T paths from pelitic schists and greenstones in the southwest Tauern Window, Eastern Alps. J. Metamorphic Geol., 3, 439-465.

Selverstone, J., Spear, F. S., Franz, G., & Morteani, G. 1984: High pressure metamorphism in the SW Tauern Window, Austria: P-T paths from hornblende-kyanite-staurolite schists. J.Petrology, 25, 501-531.

Spear, F. S. & Selverstone, J. 1983: Quantitative P-T paths from zoned minerals: Theory and tectonic applications. Contrib. Mineral. Petrol., 83,348-357.

Sharp, Z. D. & Ulmer, P. 1993: Stable isotope geochemistry of the aluminosilicates. Geol. Soc. Amer. Annual meeting, Boston Ma, Oct. 25-28., 100 p.

Shumacher, J. C. 1991: Empirical ferric iron corrections necessity, assumptions, and effects on selected geothermobarometers. Mineral. Mag., 55, 3 -18.

Shumacher, J. C. 1997: Appendix 2. The estimation of the proportion of ferric iron in the electron - microprobe analysis of amphiboles. Canad. Mineralogist, 35, 238 - 246.

Spear, F.S. & Franz, G. 1986: P-T evolution of metasediments from the Eclogite Zone, south central Tauern Window, Austria. Lithos, 19, 219-234.

Spear, F. S. & Rumble, D. 1986: Pressure, temperature and structural evolution of the Orfordville Belt, west-central New Hampshire. J. Petrology, 27, 1071-1093.

Thompson, J. B. Jr. 1957: The graphical analysis of mineral assemblages in pelitic schists. Amer. Mineralogist, 42, 842 - 858.

Thompson, A.B. 1976: Mineral reactions in pelitic rocks: I. Prediction of P-T-X (Fe-Mg) phase relations. Amer. J.Sci., 276, 401-424.

Thompson, A.B. & England, P.C. 1984 : Pressure-temperature-time paths of regional metamorphism II: Their inference and interpretation using mineral assemblages in metamorphic rocks. J. Petrology, 25, 894 - 928.

Uhlig, V. 1898: Geologie des Tatragebirges I. Denkschr. Ak. Wiss. Math., 64, 643-684.

Uhlig, V. 1903: *Bau und Bild der Karpaten*. F.Tempsky Verlag, Wien, 911 p.

Vozárová, A. 1998: Late Hercynian development in the Central Western Carpathians. p.41-45. In: Rakús, M. ed., 1998 : *Geodynamic development of the Western Carpathians*. Dionýz Štúr Publishers, Bratislava, 290 p.

Zeck, H.P., Monié, P.,Villa, I.M. & Hansen, B.T. 1992: High rates of cooling and uplift in the Betic Cordilleras, S.Spain. Alpine lithospheric slab detachment, mantle diapirism and extensional tectonics. Geology, 20, 79-82.